

The current-voltage characteristics of semiconductor-electrolyte junction photovoltaic cells

Cite as: Appl. Phys. Lett. **36**, 574 (1980); <https://doi.org/10.1063/1.91551>

Published Online: 23 July 2008

J. Reichman



View Online



Export Citation

ARTICLES YOU MAY BE INTERESTED IN

[Photoelectrolysis and physical properties of the semiconducting electrode WO₂](#)

Journal of Applied Physics **48**, 1914 (1977); <https://doi.org/10.1063/1.323948>

[Detailed Balance Limit of Efficiency of p-n Junction Solar Cells](#)

Journal of Applied Physics **32**, 510 (1961); <https://doi.org/10.1063/1.1736034>

[A model for the current-voltage curve of photoexcited semiconductor electrodes](#)

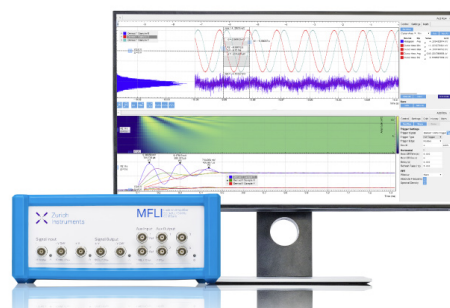
Journal of Applied Physics **48**, 4292 (1977); <https://doi.org/10.1063/1.323417>

Challenge us.

What are your needs for periodic signal detection?



Zurich
Instruments



because M_{ac} is given by⁸ $M_{ac} = M/[1 + (M\omega\tau)^2]^{1/2}$, where ω is the angular frequency and τ the intrinsic response time of 5×10^{-12} sec.⁹ Excess noise factors F , were therefore studied as a function of dc multiplication factors in the range from 5 to 50. Optimum gains in practical communication systems are typically around 10. The wavelength $\lambda \sim 1.3 \mu\text{m}$ (light-emitting diode) was used to excite the avalanche process. The spot size of the illuminated light was about $100 \mu\text{m}$ and was small in comparison with the diameter of the active region ($150 \mu\text{m}$). The experimental results are shown in Fig. 5. Values of $F \approx 7$ at $M = 10$ are obtained for n^+-n-p diodes, whereas $F \approx 10$ for n^+-p ones. Noise reduction of about 1.5 dB is achieved by the n^+-n-p structure in comparison with an n^+-p one. Excess noise factors are given by¹⁰ $F = M [1 - (1 - k_{eff}^{-1})(1 - M^{-1})^2]$, where k_{eff} is the effective ratio of hole to electron ionization coefficients. At $\lambda \sim 1.3 \mu\text{m}$ values of k_{eff} are 1.6 for n^+-n-p diodes and 1 for n^+-p ones.

Excess noise factors were also studied at $\lambda \sim 0.83 \mu\text{m}$. The results obtained are shown in Fig. 6. Values of $F \approx 6.5$ at $M = 10$ are obtained for n^+-n-p diodes, whereas $F \approx 9$ for n^+-p ones. A decrease of F values compared with the results at $\lambda \sim 1.3 \mu\text{m}$ is due to the fact that purer hole injection is achieved by illuminating with wavelengths of higher absorption coefficient for Ge.

The response speed of n^+-n-p and n^+-p diodes was studied in the frequency range up to 500 MHz by using a sinusoi-

dally modulated light of an InGaAsP laser ($\lambda = 1.3 \mu\text{m}$). The results obtained for a multiplication factor of 10 are shown in Fig. 7. The deterioration of response at 500 MHz is about 3 dB for n^+-n-p diodes and about 1 dB for n^+-p diodes. This difference is assumed to be the effect of a carrier diffusion in the n layer (see Fig. 2).

In conclusion, n^+-n-p Ge APD's have for the first time been fabricated and tested. At $\lambda \sim 1.3 \mu\text{m}$ excess noise factors are about 7 at $M = 10$ and the internal quantum efficiency is 70–80%. The 3-dB bandwidth at $M = 10$ is about 500 MHz.

The authors would like to thank Dr. Y. Mizushima, Dr. T. Kimura, and Dr. H. Kanbe for their continuing guidance and encouragement. They would also like to acknowledge useful discussions with Dr. T. Misugi and Dr. H. Takanashi.

¹H. Melchior and W.T. Lynch, IEEE Trans. Electron. Devices ED-13, 829 (1966).

²T. Kaneda and H. Takanashi, Jpn. J. Appl. Phys. 12, 1652 (1973).

³H. Ando, H. Kanbe, T. Kimura, T. Yamaoka, and T. Kaneda, IEEE J. Quantum Electron. QE-14, 804 (1978).

⁴T. Kaneda, H. Fukuda, T. Mikawa, Y. Banba, Y. Toyama, and H. Ando, Appl. Phys. Lett. 34, 866 (1979).

⁵S.L. Miller, Phys. Rev. 99, 1234 (1955).

⁶B.T. Dai and C.Y. Chang, J. Appl. Phys. 42, 5198 (1971).

⁷W.C. Dash and R. Newman, Phys. Rev. 99, 1151 (1955).

⁸R.B. Emmons, J. Appl. Phys. 38, 3705 (1967).

⁹T. Kaneda and H. Takanashi, Jpn. J. Appl. Phys. 12, 1091 (1973).

¹⁰R.J. McIntyre, IEEE Trans. Electron. Devices ED-13, 164 (1966).

The current-voltage characteristics of semiconductor-electrolyte junction photovoltaic cells

J. Reichman

Research Department, A01-26, Grumman Aerospace Corporation, Bethpage, New York 11714

(Received 12 November 1979; accepted for publication 28 January 1980)

Equations are derived giving the current-voltage characteristics of photovoltaic cells based on the semiconductor-electrolyte junction. Recombinations in the neutral region and space-charge region are included. It is shown that the rate-limiting effect of charge transfer across the interface enhances the recombination rate in these regions with increasing voltage, thereby reducing the fill factor. Significant differences in the behavior of these cells and other photovoltaic cells are pointed out.

PACS numbers: 72.40.+w, 85.30.De, 73.40.Mr, 85.80.Fi

There has been strong interest shown recently in the photovoltaic behavior of semiconductor-electrolyte junction cells owing to their potential for low cost and good efficiency in converting light to electricity or in producing useful chemicals. Although considerable experimental studies of the characteristics of various semiconductor-electrolyte junctions have been reported,^{1,2} there has been comparatively little theoretical work advanced concerning the analysis and interpretations of their current-voltage (J - V) characteristics.

Dewald³ derived expressions for the J - V characteristics of semiconductor-electrolyte cells by assuming all incident photons are absorbed in the space-charge region (SCR). Photogeneration of carriers in the neutral region and recombinations in the SCR were neglected. Wilson⁴ includes neutral-region photogeneration in this model as well as interface recombinations. He neglects SCR recombinations and the effect of the opposing dark current. The resulting equations are fairly complex but can be reduced to a form similar to Eq. (8) in this letter. Reiss⁵ derives J - V equations for various

model cases. Rather than assuming quasiequilibrium conditions in the SCR, he integrates the transport equation by neglecting SCR recombinations. The resultant J - V equations contain terms requiring numerical integration making them somewhat difficult to use.

In this letter J - V equations are derived that can be easily used to predict and analyze the performance characteristics of semiconductor-electrolyte junction photovoltaic devices. Important differences between these devices and conventional p - n junction or Schottky barrier photovoltaic devices are pointed out. **In particular, the importance of neutral-region and SCR recombinations due to rate-limiting effects of charge transfer kinetics are discussed and illustrated.**

A semiconductor in contact with an electrolyte forms a barrier due to the difference in Fermi levels of the two phases. This is shown in Fig. 1 which is an energy-level diagram under illumination for a model junction consisting of an n -type semiconductor electrode in contact with a redox electrolyte. The electrolyte Fermi level is determined by the redox potential of the acceptor ions A^{2+} and donor ions A^+ . A voltage V is assumed to be created due to the incident photon flux displacing the electron quasi-Fermi level of the semiconductor upward in the forward bias direction. The potential drop across the Helmholtz layer at the interface is assumed constant with changes in voltage due to incident photons or applied bias. This is good approximation because of the small thickness of the Helmholtz layer compared to the semiconductor SCR thickness.¹ All changes in voltage then appear as changes in potential drop across the SCR or $\phi_b = \phi_{b0} - V$ where ϕ_{b0} is the equilibrium band bending voltage. The width of the SCR in the depletion approximation is given by $W = (2\epsilon\epsilon_0\phi_b/qN)^{1/2}$ where ϵ is the dielectric constant, ϵ_0 is the permittivity of free space, q is the electron charge and N is the carrier density.

The distribution of energy states of the redox ions are broadened as shown in Fig. 1 owing to the thermal fluctuations of the solvation structure.⁶ Charge transfer from semiconductor states to ion states only occurs when there is overlap of occupied and unoccupied energy levels owing to energy conservation. The equations for currents due to charge transfer across the interface can be written in the following form³:

$$J_n = -I_n^0 [n_s/n_{s0} - 1], \quad (1)$$

$$J_p = I_p^0 [p_s/p_{s0} - 1], \quad (2)$$

where the electron and hole current densities J_n and J_p are given as functions of the ratio of their interface concentration n_s and p_s to their equilibrium interface concentration n_{s0} and p_{s0} . The electron and hole exchange current parameters I_n^0 and I_p^0 are determined by the degree of overlap of semiconductor band and interface states with the redox ion states and by the transition probabilities for charge transfer.⁶ These equations assume that the charge transfer reactions are kinetically first order with respect to the electron and hole densities at the interface and that the ion concentrations at the interface are constant. The latter assumption is equivalent to assuming sufficiently rapid mass transfer in the electrolyte that concentration polarization effects are negligible.

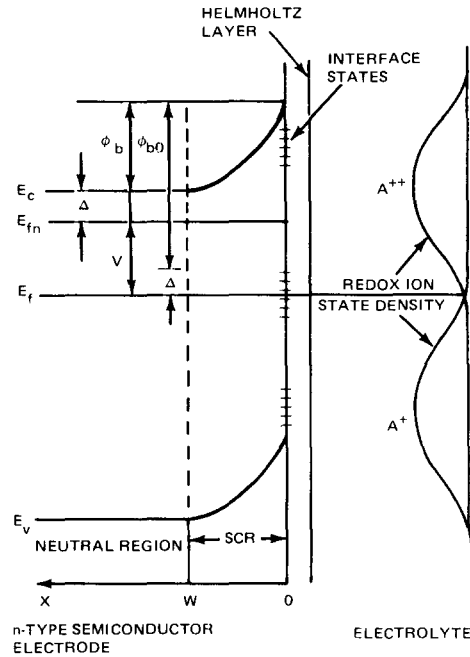


FIG. 1. Energy-level diagram for an n -type semiconductor-electrolyte junction under illumination. The electron quasi-Fermi level E_{fm} is displaced from the equilibrium Fermi level E_f owing to the photovoltage V . The band bending voltage ϕ_b is also shown changed from its equilibrium value ϕ_{b0} by the photovoltage.

To determine the current densities, the carrier densities at the interface must be determined. For the hole density this is done by solving the diffusion equation for minority carriers in the neutral region of the semiconductor.

$$D \frac{d^2 p}{dx^2} - \frac{p - p_0}{\tau} + I_0 \alpha \exp(-\alpha x) = 0, \quad (3)$$

where D is the diffusion coefficient, τ is the lifetime, α is the absorption coefficient, p_0 is the equilibrium hole density, and I_0 is the monochromatic photon flux incident on the semiconductors after all corrections for interface reflections and electrolyte absorption losses have been made. The hole current density at the depletion edge, J_w , is obtained from the solution to the above equation by using the boundary conditions $p = p_0$ at $x = \infty$ and $p = p_w$ at $x = W$:

$$J_w = -J_0(p_w/p_0 - 1) + qI_0\alpha L \exp(-\alpha W)/(1 + \alpha L), \quad (4)$$

where J_0 is the saturation current density as given by $J_0 = qp_0L/\tau$, p_0 is given by $p_0 = n_i^2/N$, n_i is the intrinsic carrier density, and L is the hole diffusion length. The above solution is a good approximation for finite electrodes where the neutral-region thickness is greater than a diffusion length.

To obtain relations between the carrier density at the interface and at the depletion edge, the quasiequilibrium approximation is made.⁷ This assumes that the electrons and holes are separately in translational equilibrium. For the nondegenerate case considered here the following relations then apply:

$$n_s = n_w \gamma_1 \exp(-q\phi_b/kT), \quad (5)$$

$$p_s = p_w \gamma_2 \exp(+q\phi_b/kT), \quad (6)$$

where the terms γ_1 and γ_2 are constants that give the ratio of energy states at the interface to that of the bulk. The additional interface states are those near the band edges that are available for charge transfer and are assumed in equilibrium with the band states. States at energy levels near midgap are excluded from this and should be treated separately as recombination centers.

If, initially, recombinations in the SCR and at the interface are neglected, the hole current transferred across the interface, J_p , is equal to the sum of the current density at the depletion edge, J_w , and the current density in the SCR generated by photon absorption given by

$$J_{SCR}^G = qI_0[1 - \exp(-\alpha W)], \quad (7)$$

By equating the components of the hole currents given by Eq. (4) and (7) to the total hole current J_p as given by Eq. (2) and using Eq. (6) an expression for the ratio p_s/p_{s0} is found and then substituted into Eq. (2) to give

$$J_p = \frac{J_g - J_0 \exp(qV/kT)}{1 + J_0 \exp(qV/kT)/I_p^0}. \quad (8)$$

The term J_g in the numerator of Eq. (8) is given by

$$J_g = J_0 + qI_0[1 - \exp(-\alpha W)/(1 + \alpha L)], \quad (9)$$

This expression was obtained by Gartner⁸ for the photocurrent of a Schottky barrier photodiode in reverse bias. It was obtained from the sum of Eqs. (7) and (4) by assuming $p_w = 0$. This is in contrast to the method given here, where p_w is obtained in a manner consistent with the interface boundary conditions. Despite this limitation on its application, the Gartner model has been used to analyze the photocurrents of semiconductor electrolyte barrier devices.^{9,10}

The unique feature of the semiconductor-electrolyte junction is contained in the denominator of Eq. (8). When the voltage becomes large enough so that the expression $J_0 \exp(qV/kT)/I_p^0$ is of the order of 1, then the hole current starts to rapidly decrease as the voltage increases. A simple physical interpretation of this can be given. As the voltage increases, the band bending decreases and therefore the hole concentration at the depletion edge approaches the interface hole concentration as shown by Eq. (6). Since the recombination rate in the neutral region increases with excess hole concentration, the result is a decrease in hole current across the interface. The role of the kinetics of charge transfer across the interface can now be seen. Slower kinetics are reflected in smaller values of I_p^0 . This then requires higher interface hole densities to achieve a given current density as seen by Eq. (2). The corresponding hole density in the neutral region would then be higher for a given voltage leading to higher recombination rates. For practical purposes it is therefore desirable to maximize the value of I_p^0 to increase the fill factor and thus yield higher efficiencies.

An additional effect is the opposing current due to majority carrier electron transfer from the conduction band to acceptor ions in the electrolyte. This current can be deter-

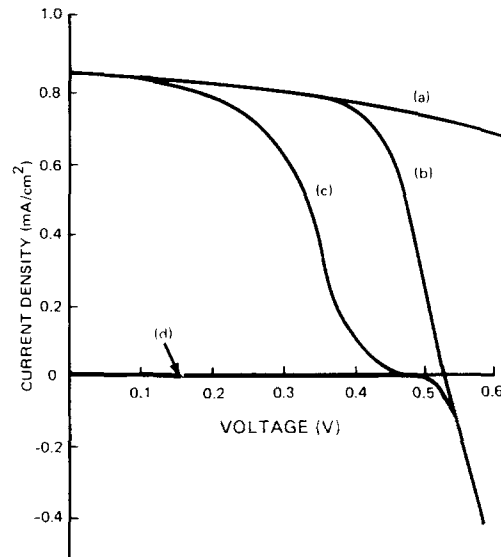


FIG. 2. Comparison of calculated J - V characteristics of semiconductor-electrolyte junction device under illumination of 1 mA/cm^2 photon flux. Parameters used were $I_p^0 = 10^{-5} \text{ mA/cm}^2$, $I_n^0 = 10^{-10} \text{ mA/cm}^2$, $L = 0.5 \times 10^{-4} \text{ cm}$, $N = 10^{16} \text{ cm}^{-3}$, $\alpha = 3 \times 10^4 \text{ cm}^{-1}$, $n_i = 10^7 \text{ cm}^{-3}$, $\epsilon = 12$, $\phi_{b0} = 0.7 \text{ V}$, $\tau = 10^{-9} \text{ sec}$. Curves are calculated from (a) the Gartner model, Eq. (9); (b) Eqs. (8) and (10), including bulk recombinations; (c) Eqs. (10) and (11), including SCR recombinations; and (d) the dark-current Eqs. (8) and (10) with $I_0 = 0$.

mined by using Eq. (5) in Eq. (1) to give

$$J_n = -I_n^0 [\exp(qV/kT) - 1]. \quad (10)$$

To obtain the above, the electron density at the depletion edge is assumed constant with voltage. This is a reasonable approximation at the low-level injection conditions considered here. The total current density is then given by the sum of Eqs. (8) and (10).

The effects of recombinations in the SCR on the J - V characteristics was determined by using the method of Sah, Noyce, and Shockley^{11,12} to calculate the SCR recombination current J_{SCR}^R . The result is $J_{SCR}^R = K(p_s/p_{s0})^{1/2}$, where $K = \pi k T n_i W \exp(qV/2kT)/4\tau\phi_b$. By equating the components of the hole fluxes, as previously, the following equation for the interface hole concentration was then found.

$$p_s/p_{s0} = \{ [-K + (K^2 + 4AB)^{1/2}] / 2A \}^2, \quad (11)$$

where $A = I_p^0 + J_0 \exp(qV/kT)$ and $B = I_p^0 + J_g$. The hole current J_p is then found by substituting Eq. (11) into Eq. (2).

A comparison of the J - V characteristics using the equations given here for different levels of approximation is shown in Fig. 2. The parameters are given in the caption and are representative of somewhat defective n -GaAs. Curve (a) is for the lowest order of approximation as given by the Gartner model [Eq. (9)]. The decrease in current with voltage results from the reduction in SCR width, causing greater recombinations in the neutral region. Curve (b) calculated from Eqs. (8) and (10), includes the above effect and in addition includes the opposing dark current and the increasing recombination rate in the neutral region due to minority car-

rier buildup caused by the rate limiting effect of interface charge transfer. Curve (c) as obtained from Eqs. (10) and (11) includes all of the above effects plus recombinations in the SCR. The results indicate that for low voltage the Gartner model gives the same results as the more general models. With increasing voltage, however, there are significant differences in the results as the other loss mechanisms become important. It is seen that SCR recombinations are quite significant and dominate the J - V characteristics at higher voltages. This result differs from that of Schottky barrier or p - n junction solar cells where SCR recombinations of photogenerated carriers can usually be neglected.¹³ In these devices transport of minority carriers across the barrier is not usually rate limited; therefore minority carrier accumulation in the SCR does not occur. Curve (d) for the dark current ($I_0 = 0$) is seen to show quite low currents until the voltage exceeds 0.5 V. This is due to the small overlap of conduction-band states with ion acceptor states resulting in low values of I_n^0 . This result is also quite different from other photovoltaics, where larger dark currents often account for the most significant reduction in current with voltage.¹³

In conclusion, equations have been derived for the J - V characteristics of semiconductor-electrolyte photovoltaics where the effects of rate-limiting interface charge transfer

have been included. It has been shown that SCR recombinations can be a quite significant loss mechanism and cannot generally be neglected. The significance of effects not included here such as interface recombinations and mass transfer limitations can be answered by detailed analysis of specific experiments using well-characterized electrodes.

¹A.J. Nozik, in *Annual Reviews in Physical Chemistry* (Annual Reviews, Palo Alto, 1978) Vol. 29, p. 189.

²L.A. Harris and R.H. Wilson, in *Annual Reviews in Material Science* (Annual Reviews, Palo Alto, 1978), Vol. 8, p. 99.

³J.F. Dewald, in *Semiconductors* (Reinhold, New York, 1959), p. 727.

⁴R.H. Wilson, *J. Appl. Phys.* **48**, 4292 (1977).

⁵H. Reiss, *J. Electrochem. Soc.* **125**, 937 (1978).

⁶H. Gerischer, in *Physical Chemistry, An Advanced Treatise* (Academic, New York, 1970), Vol. 9A, p. 463.

⁷F. Berz, *J. Appl. Phys.* **50**, 4479 (1979).

⁸W.W. Gartner, *Phys. Rev.* **116**, 84 (1959).

⁹M.A. Butler, *J. Appl. Phys.* **48**, 1914, (1977).

¹⁰J.H. Kennedy and K.W. Frese, Jr., *J. Electrochem. Soc.* **125**, 723 (1978).

¹¹C.T. Sah, R.N. Noyce, and W. Shockley, *Proc. IRE* **45**, 1228 (1957).

¹²C.H. Henry, R.A. Logan, and F.R. Merritt, *J. Appl. Phys.* **44**, 3530 (1978).

¹³H. Hovel, *Semiconductor and Semimetals, Vol. 11, Solar Cells* (Academic, New York, 1975).

Effect of lattice misfit on pn junction characteristics

K. Ito

Department of Electronics, Faculty of Engineering, Shinshu University, Nagano 380, Japan

(Received 4 September 1979; accepted for publication 23 January 1980)

Junction diodes of $p^+ \text{Si}_{1-x}\text{Ge}_x$ - $n \text{Si}$ ($0 \leq x \leq 0.2$) were made by a liquid-phase epitaxial method. A lattice misfit larger than 0.3% present at the junction interface caused an increase of the current density at small forward bias and also a weak voltage dependence of the current at large forward bias. The forward I - V characteristics were explained in terms of carrier recombination generation in the space-charge region of an asymmetrical pn junction.

PACS numbers: 73.40.Lq, 61.70.Ng, 81.15.Lm, 85.30.De

In Ge/Si heteroepitaxy which has a lattice mismatch of 4.2%, misfit dislocations exist at the interface even if the average thickness of the deposited Ge layer is several tens of nanometers.¹ Dislocation generation in epitaxial Si layers deposited on Si substrates can also occur for a small lattice misfit less than 0.2%, which in turn is the result of doping difference.² The misfit dislocations might have some effects on the electrical properties of Si pn junctions produced by epitaxy. In this letter, I investigate the effects of the lattice misfit up to 0.8% which is present at the junction interface, controlling the lattice constants of the epitaxial layers. It was found that the forward I - V characteristics of the Si pn junctions were significantly altered by the presence of a lattice misfit larger than 0.3%.

A vertical solution-growth system was used to deposit epitaxial p -type $\text{Si}_{1-x}\text{Ge}_x$ alloy layers about 50 μm thick on n -type Si (111) substrates whose resistivity was 0.4–12 $\Omega \text{ cm}$. Predetermined amounts of Al (99.999% pure) as a solvent together with Si and Ge were contained in either a

carbon or an alumina crucible. The seed crystal was melted back to be etch cleaned in the solution just prior to the deposition. The growth was continued for 15 min, during which the temperature was allowed to fall with a cooling rate of 1 $^\circ\text{C}/\text{min}$. The seed was then pulled out from the solution. A relation between the solid alloy composition x and the melt composition at 1000 K is shown in Table I. The melt which had initially had one of the above compositions and had been used for the first growth run was reused for several subsequent growth runs at elevated temperatures. Increasing growth temperature by 5 K between the two consecutive runs, we were able to obtain epitaxial alloy layers with a composition nearly equal to that of the first growth.

We controlled the misfit at the junction interface up to 0.8% by changing the atomic fraction x of epitaxial $\text{Si}_{1-x}\text{Ge}_x$ alloy layers up to 0.2. The lattice misfit is defined by

$$m = (a_2 - a_1)/a_1, \quad (1)$$

where a_1 (a_2) is the lattice constant of Si ($\text{Si}_{1-x}\text{Ge}_x$). Since